Inorganic/organic composite fluorinated interphase layers for stabilizing ether-based electrolyte in high-voltage lithium metal battery

Qimeng Ren[a], Qinglei Wang[b*], Li Su[b], Guodong Liu[b], Yan Song[b], Xuehui Shangguan[b*], Faqiang Li[b*]

a. School of Chemistry & Chemical Engineering, Linyi University, Linyi 276005, China

b. School of Materials Science and Engineering, Linyi University, Linyi 276003, China

*Corresponding author.

Corresponding author E-mail: shangguanxuehui@lyu.edu.cn (Xuehui Shangguan); wangqinglei@lyu.edu.cn (Qinglei Wang); lifaqiang@lyu.edu.cn (Faqiang Li)

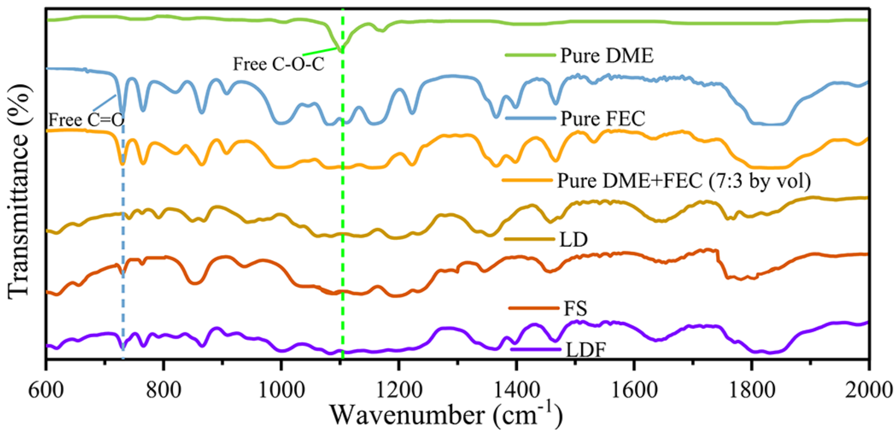

Fig. S1 FTIR spectra of different solvents and electrolytes.

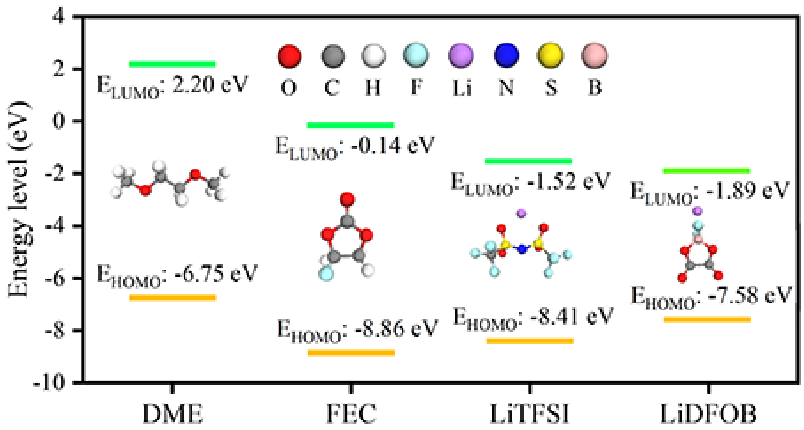

Fig. S2 Calculated HOMO and LUMO of the solvents and Li salts.

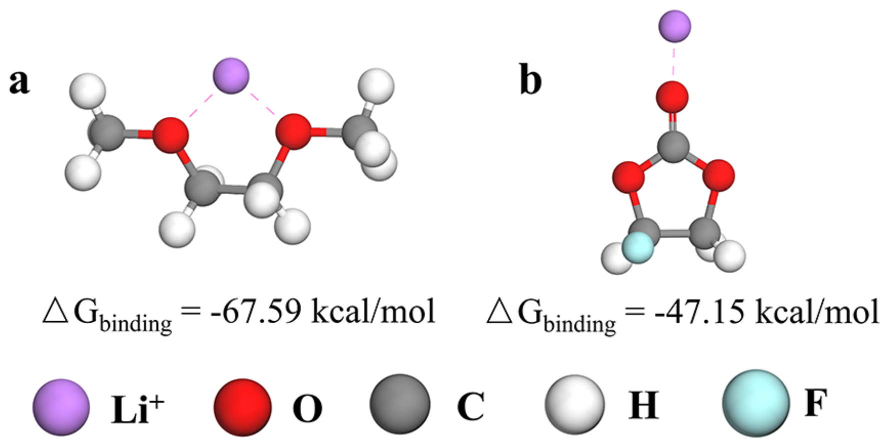

Fig. S3 The binding energy of (a) Li^+-DME and (b) Li^+-FEC.

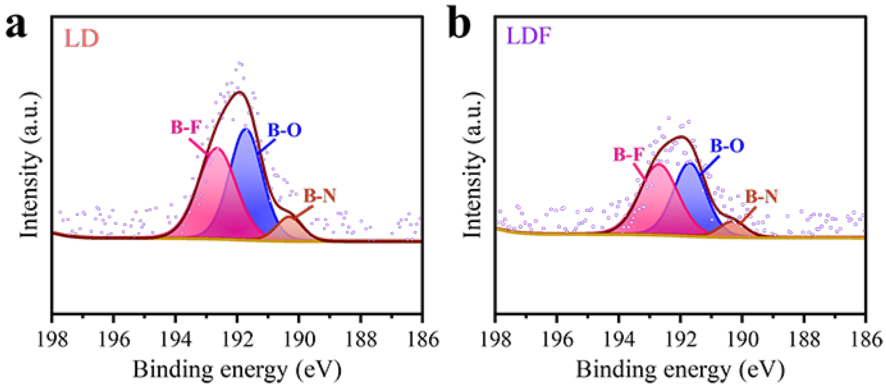

Fig. S4 B 1s XPS profiles of the $LiCoO_2$ cathode in Li/$LiCoO_2$ cells with the (a) LD and (b) LDF electrolytes after 100 cycles.

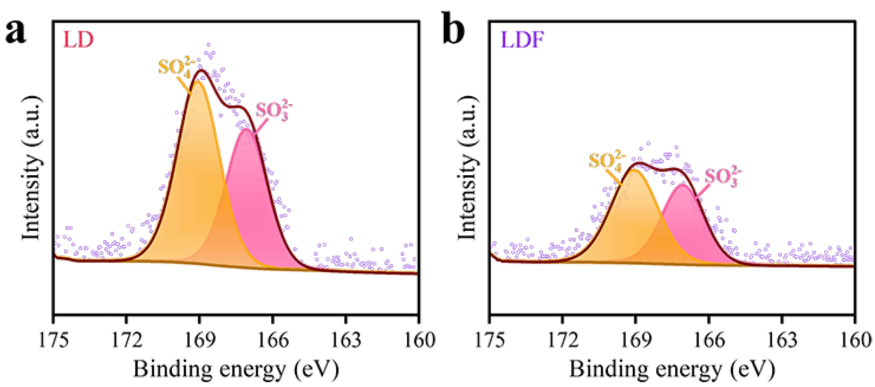

Fig. S5 S 2p XPS profiles of the $LiCoO_2$ cathode in Li/$LiCoO_2$ cells with the (a) LD and (b) LDF electrolytes after 100 cycles.

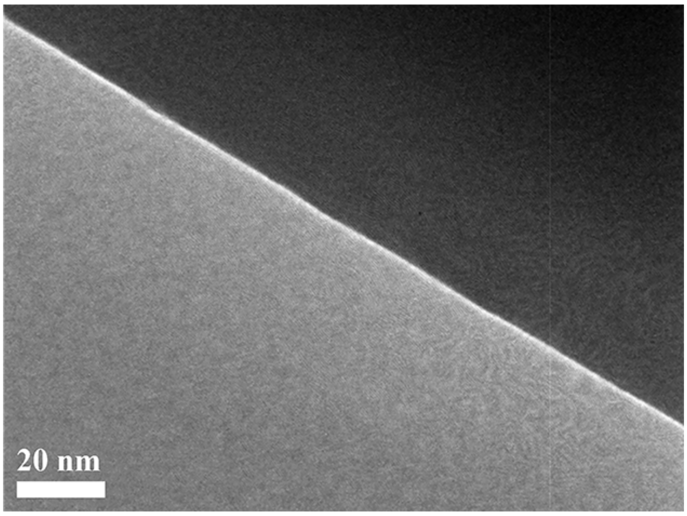

Fig. S6 TEM morphologies of pristine $LiCoO_2$ cathode

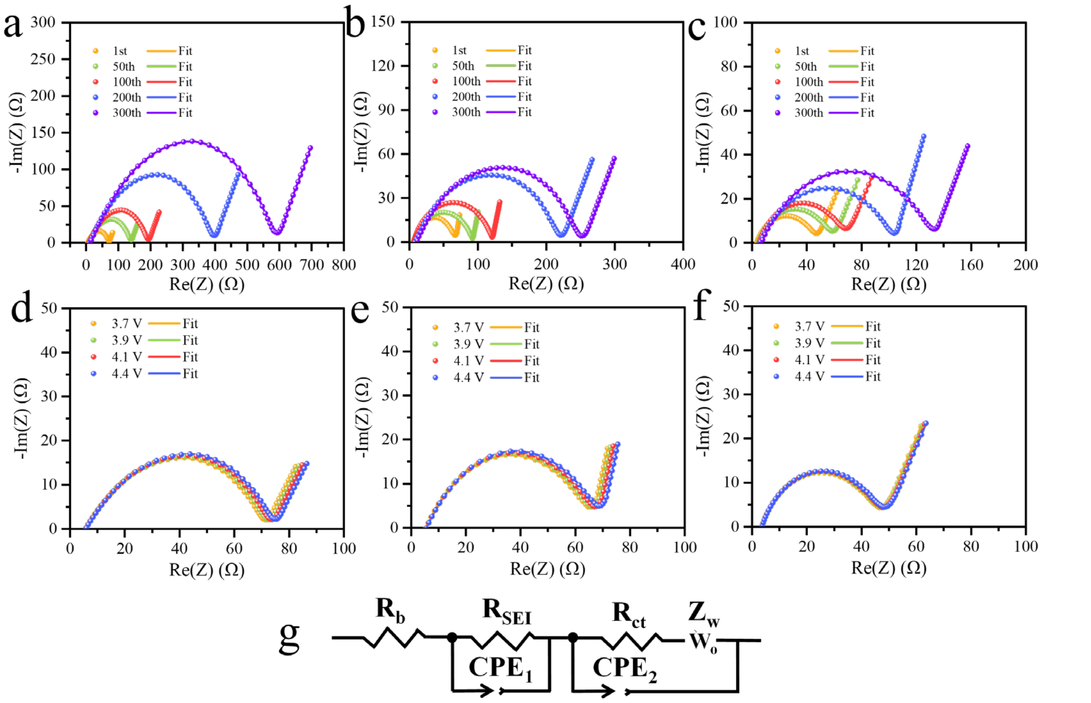

Fig. S7 (a-c) Electrochemical impedance spectra (EIS) of the Li/LCO cells after different cycles. All data were collected at fully discharged state of the cells. (d-f) Impedance changes during charging process. (a,d) E-control-1, (b,e) LD and (c,f) LDF electrolyte. (g) The corresponding equivalent circuit.

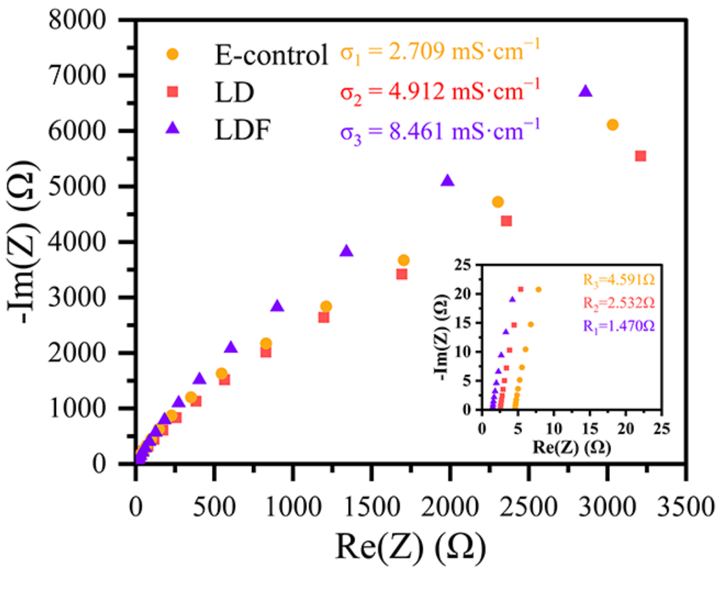

Fig. S8 Ionic conductivity for E-control, LD, and LDF electrolytes.

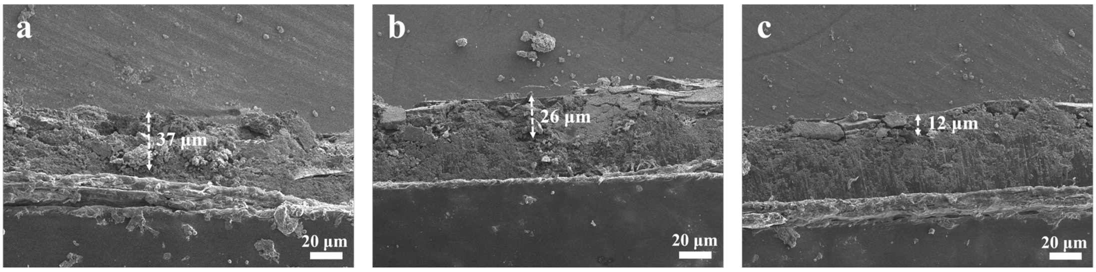

Fig. S9 Cross-sections SEM images of the Li metal anode in Li/LCO cells with (a) E-control-1, (b) LD and (c) LDF electrolytes after 100 cycles.

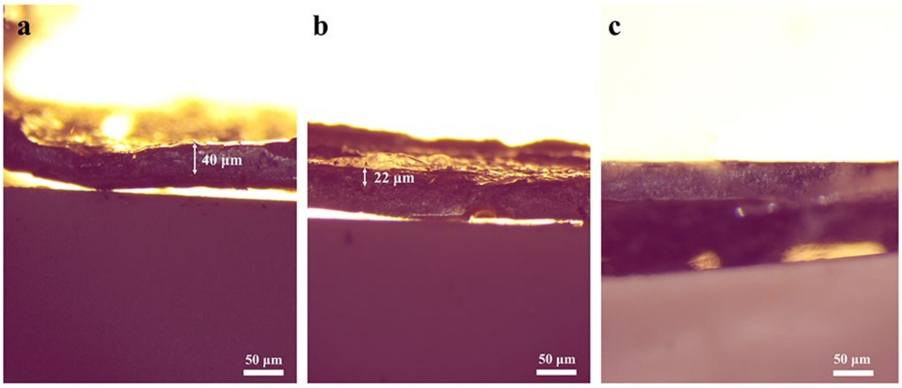

Fig. S10 Optical microscopy images of the Li metal anode in Li/LCO cells with (a) E-control-1, (b) LD and (c) LDF electrolytes after 100 cycles.

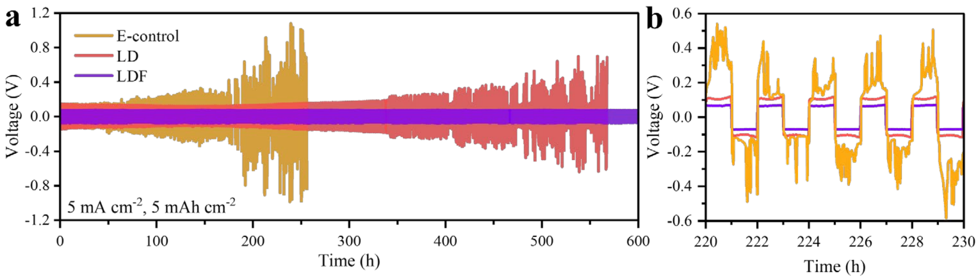

Fig. S11 (a) Cycling performance of Li/Li symmetric cell in different electrolytes with a capacity of 5 mAh cm^{-2} at a current density of 5 mA cm^{-2}. (b) Enlarged galvanostatic charge-discharge curves based on a.

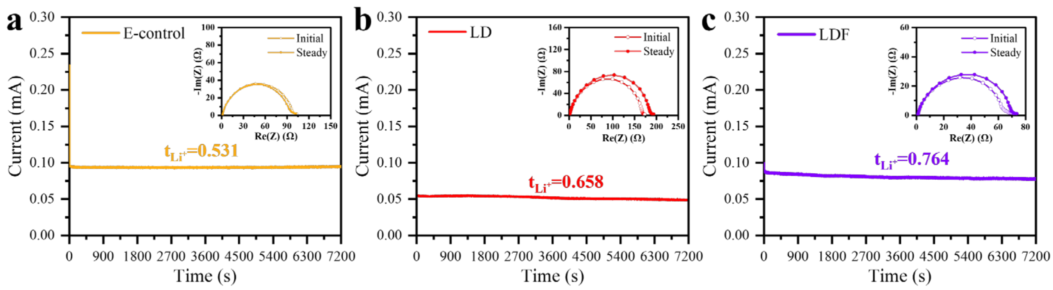

Fig. S12 Li^+ transference numbers and the chronoamperometry profiles of Li/Li symmetrical cells in (a) E-control (b) LD (c) LDF electrolytes.

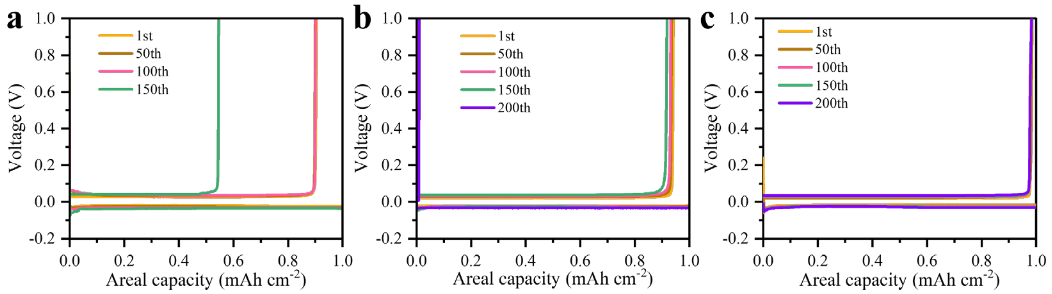

Fig. S13 Voltage profiles of Li/Cu plating/stripping processes at specific cycles in different electrolytes. (a) E-control, (b) LD, (c) LDF.

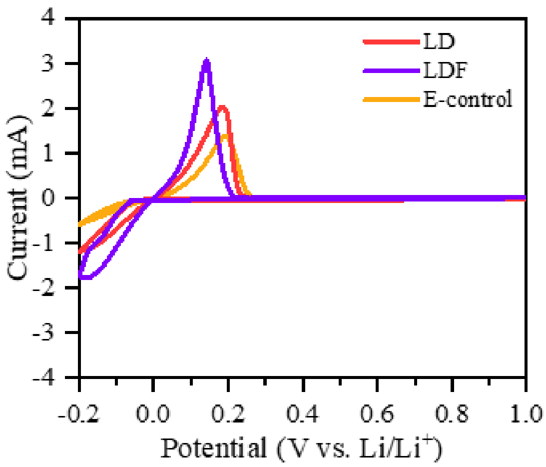

Fig. S14 CV curves of Li/Cu cells for different electrolytes.

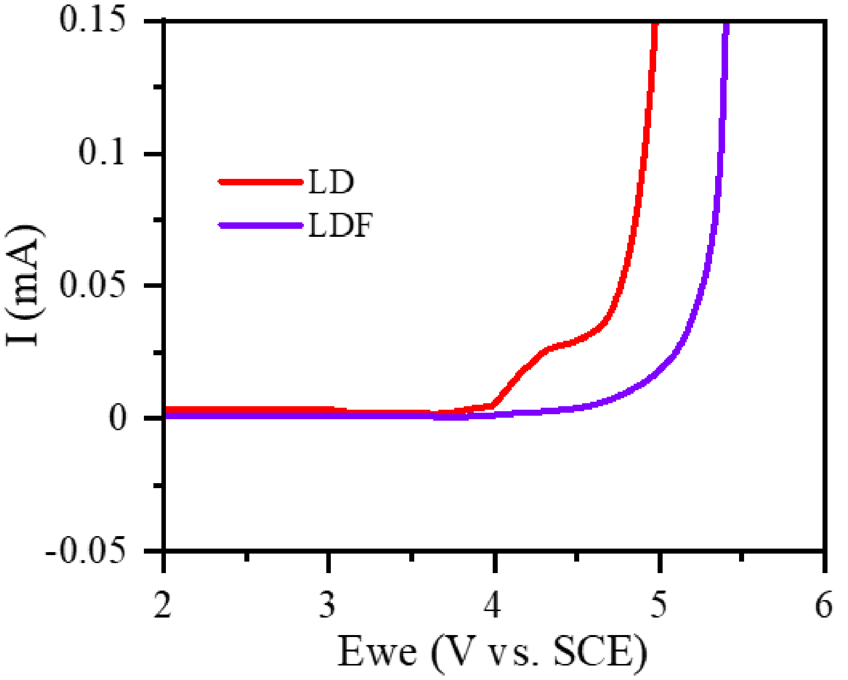

Fig. S15 Oxidation stability of electrolytes in Li/SS cells tested by linear sweep voltammetry (LSV) at a scan rate of 1 mV s^{-1}.

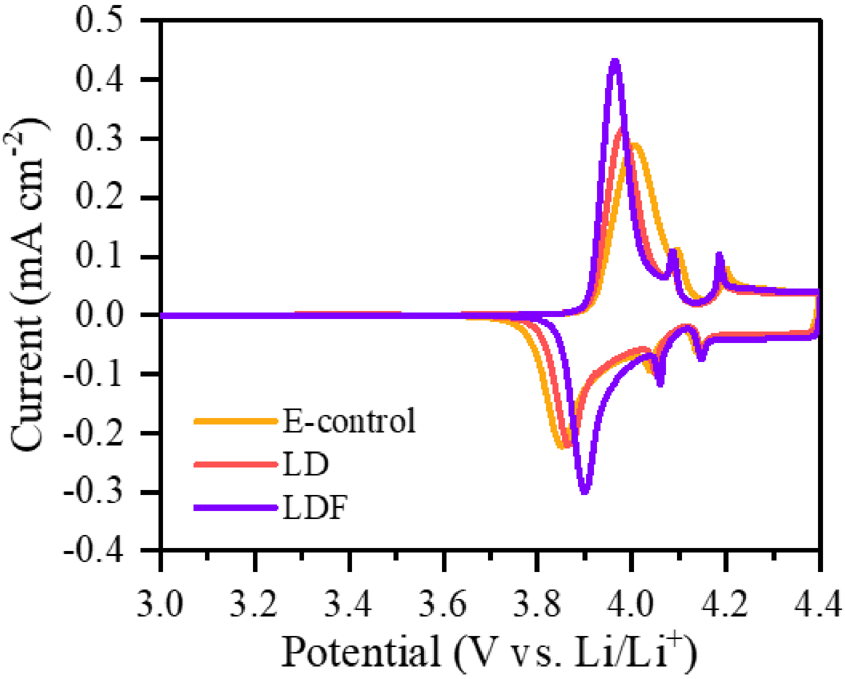

Fig. S16 CV curves of $Li/LiCoO_2$ cells for different electrolytes.

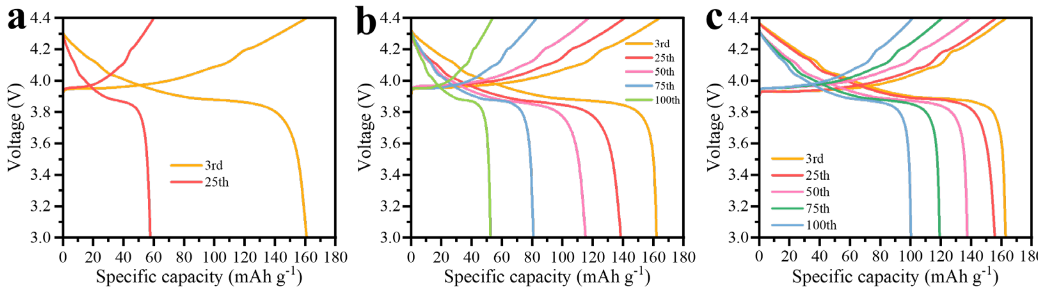

Fig. S17 Voltage profiles of Cu/ $LiCoO_2$ cells employing (a) E-control, (b) LD, (c) LDF.

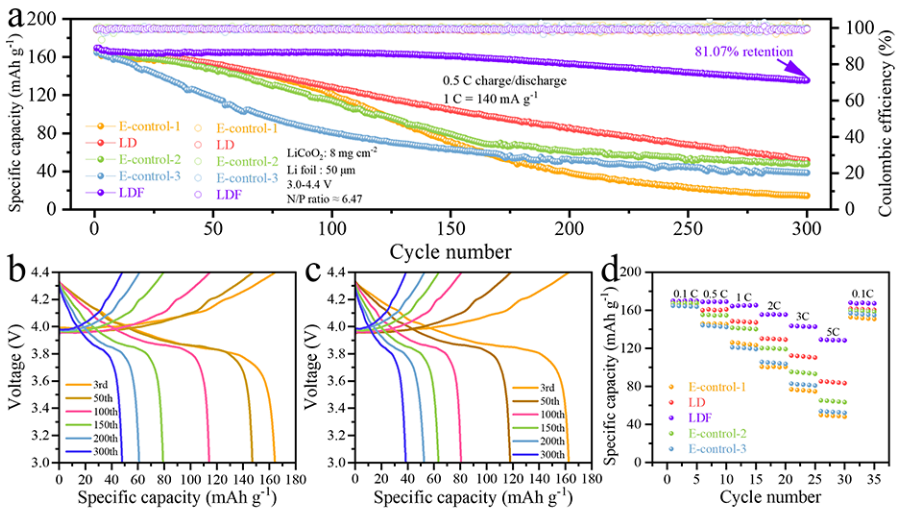

Fig. S18 (a) Long-term cycling performances of $Li/LiCoO_2$ cells. (b-c) Corresponding voltage profiles of $Li/LiCoO_2$ batteries employing different electrolytes. (b) E-control-2; (c) E-control-3. (d) Rate performances.

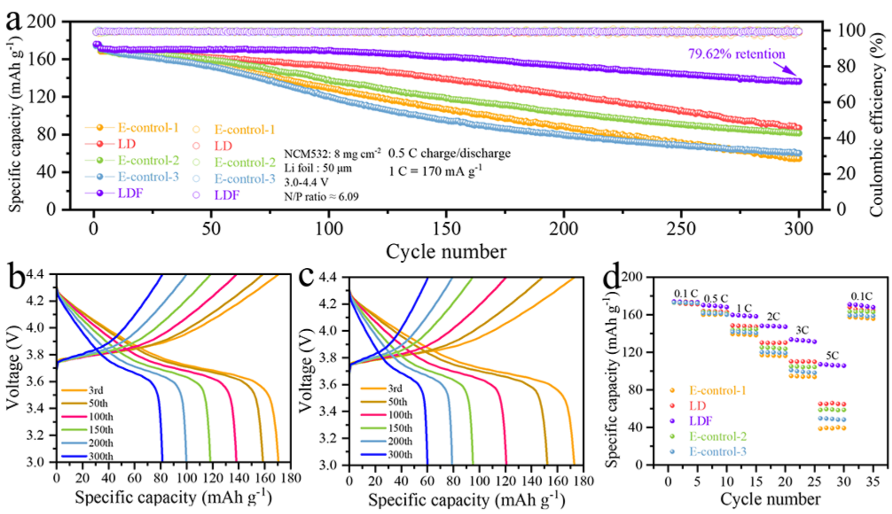

Fig. S19 (a) Long-term cycling performances of Li/NCM532 cells. (b-c)

Corresponding voltage profiles of Li/NCM532 batteries employing different electrolytes. (b) E-control-2; (c) E-control-3. (d) Rate performances.

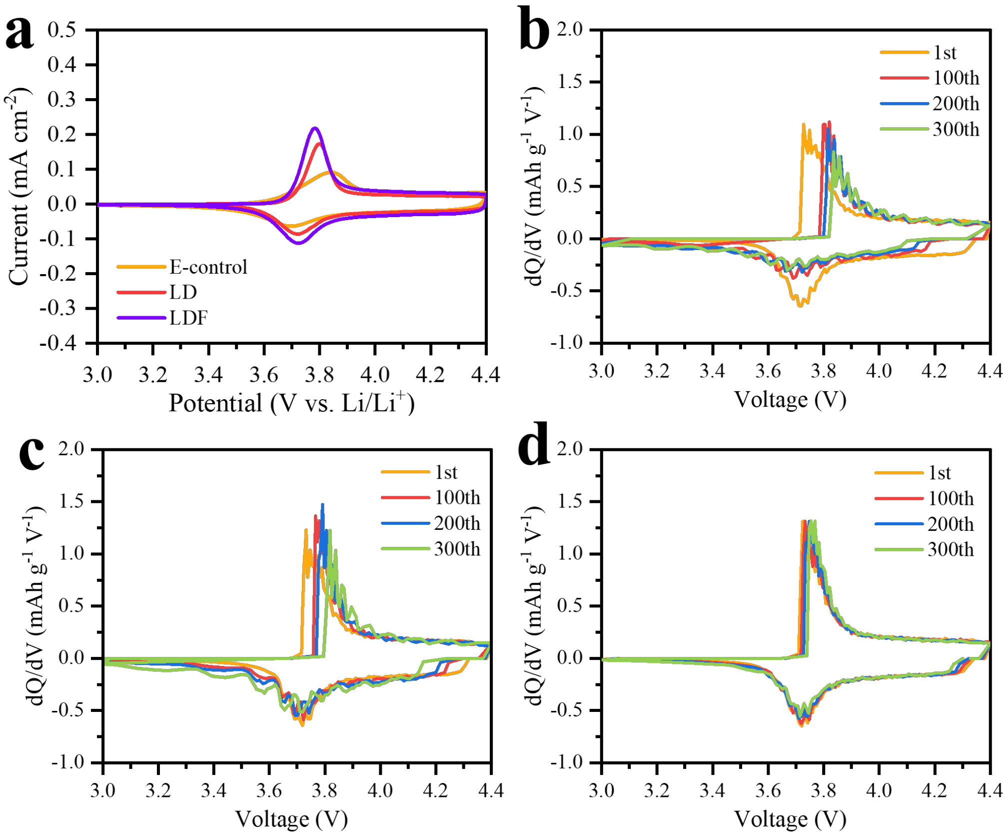

Fig. S20 (a) Cyclic voltammogram of Li/NCM532 cells in the potential region of 3.0 V−4.4 V at a scan rate of 0.05 mV s^{-1} in different electrolytes. (b-d) dQ/dV vs. V profiles of Li/NCM532 cells with different electrolytes at potential range of 3.0-4.4 V. (b) E-control-1, (c) LD and (d) LDF electrolyte.

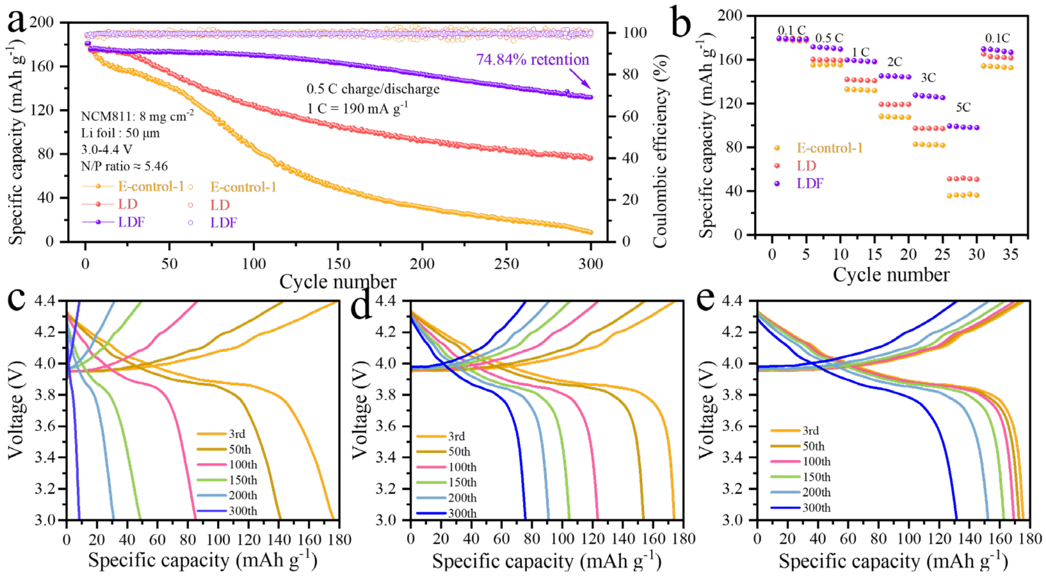

Fig. S21 (a-e) Galvanostatic cycling performance of Li/NCM811 cells. (a) Long-term cycling performances of cells. (b) rate performances. Voltage profiles of cells employing (c) E-control-1, (d) LD, (e) LDF.

Table S1. Corresponding impedance values of Figure S7 a-c.

Electrolyte system	E-control			LD			LDF		
Cycle number	Rb (Ω)	Rsei (Ω)	Rct (Ω)	Rb (Ω)	Rsei (Ω)	Rct (Ω)	Rb (Ω)	Rsei (Ω)	Rct (Ω)
1	5.73	7.55	68.70	5.33	7.34	66.81	3.99	5.18	47.14
50	8.46	15.15	137.78	6.09	10.12	92.03	4.67	6.41	58.31
100	10.02	21.28	193.50	6.32	13.28	120.77	5.61	7.46	67.83
200	13.76	43.73	397.63	10.27	24.24	220.36	7.76	11.32	102.91
300	16.41	65.307	593.70	11.59	27.57	250.72	9.55	14.49	131.89

Table. S2 Performance comparison and summary of lithium metal batteries with different conditions and electrolytes in the reported researches.

Electrolyte composition	Li Anode thickness	Cathode	Voltage range	N/P ratio	Electrochemical performance	Ref
LiFSI-1.2 DME	50 μm	NCM811	2.8~4.4 V	2.2	80% 65 cycles	1
LiFSI-1.2DME+3TTE	50 μm	NCM811	2.8~4.4 V	2.38	80% 155 cycles	2
4.6 M LiFSI - 2.3 M LiTFSI-DME	150 μm	NCM622	4.4 V	21	88% 300 cycles	3
1.5 M LiFSI-8TTD-2DME	20 μm	NCM811	2.8~4.7 V	2.5	80% 100 cycles	4
1 M $LiPF_6$ + 0.65 M $LiNO_3$-FEC/DME	45 μm	NCM811	2.8~4.3 V	4.16	80% 280 cycles	5
2.0 M LiFSI+1 M LiTFSI in DME+1 wt.% LiDFBP+3 wt.% $LiNO_3$	100 μm	NCM811	3.0~4.2 V	7.5	80% 241 cycles	6
1.2 M LiFSI+0.15 M LiDFOB in EC/EMC/BTFE	50 μm	NCM333	2.7~4.3 V	2.3	84% 100 cycles	7
This work	50 μm	$LiCoO_2$	3~4.4 V	6.47	81% 300 cycles	

Reference

1. X. Cao, L. F. Zou, B. E. Matthews, L. C. Zhang, X. Z. He, X. D. Ren, M. H. Engelhard, S. D. Burton, P. Z. El-Khoury, H.-S. Lim, C. J. Niu, H. K. Lee, C. S. Wang, B. W. Arey, C. M. Wang, J. Xiao, J. Liu, W. Xu and J. G. Zhang, *Energy Storage Mater.*, 2021, **34**, 76-84.
2. X. D. Ren, L. F. Zou, X. Cao, M. H. Engelhard, W. Liu, S. D. Burton, H. Lee, C. J. Niu, B. E. Matthews, Z. H. Zhu, C. M. Wang, B. W. Arey, J. Xiao, J. Liu, J. G. Zhang and W. Xu, *Joule*, 2019, **3**, 1662-1676.
3. J. Alvarado, M. A. Schroeder, T. P. Pollard, X. Wang, J. Z. Lee, M. Zhang, T. Wynn, M. Ding, O. Borodin, Y. S. Meng and K. Xu, *Energy Environ. Sci.*, 2019, **12**, 780-794.

4. Y. Zhao, T. H. Zhou, M. El Kazzi and A. Coskun, *ACS Appl. Energy Mater.*, 2022, **5**, 7784-7790.
5. X. Wang, S. Wang, H. Wang, W. Tu, Y. Zhao, S. Li, Q. Liu, J. Wu, Y. Fu, C. Han, F. Kang and B. Li, *Adv Mater*, 2021, **33**, 2007945.
6. S. Kim, S. O. Park, M.-Y. Lee, J.-A. Lee, I. Kristanto, T. K. Lee, D. Hwang, J. Kim, T.-U. Wi, H.-W. Lee, S. K. Kwak and N.-S. Choi, *Energy Storage Mater.*, 2022, **45**, 1-13.
7. L. Yu, S. Chen, H. Lee, L. Zhang, M. H. Engelhard, Q. Li, S. Jiao, J. Liu, W. Xu and J.-G. Zhang, *ACS Energy Lett.*, 2018, **3**, 2059-2067.